Capacitance Extraction of 3-D Conductor Systems in Dielectric Media with High-Permittivity Ratios

Johannes Tausch and Jacob White, *Associate Member, IEEE*

***Abstract*— We describe a perturbation formulation for the problem of computing electrostatic capacitances of multiple conductors embedded in multiple dielectric materials. Unlike the commonly used equivalent-charge formulation (ECF), this new approach insures that the capacitances are computed accurately even when the permittivity ratios of the dielectric materials are very large. Computational results from a three-dimensional multipole-accelerated algorithm based on this approach are presented. The results show that the accuracy of this new approach is nearly independent of the permittivity ratios and superior to the ECF for realistic interconnect structures.**

***Index Terms*—Boundary-element methods, capacitance, dielectric materials.**

I. Introduction

THE boundary-element, or method-of-moments [1], technique for computing capacitances in complicated three-dimensional (3-D) geometries has rebounded in popularity in the last decade. This is due, in part, to the development of very fast solution algorithms based on sparsifying the associated dense matrices [2]–[5]. The combination of the boundary-element method and sparsification can be extended to problems with multiple dielectric materials using an equivalent-charge formulation (ECF) [6]–[8], but the approach is well known to have numerical accuracy difficulties when permittivity ratios are high [9].

If the dielectric materials form flat layers, then the problem with ECF can be avoided by using layered media Green's functions [10], [11] and appropriately modified sparsification techniques [12], [13]. For problems with arbitrarily shaped dielectric interfaces with moderate permittivity ratios, it is possible to use ECF, though for such problems, the Galerkin boundary-element method is far more accurate than centroid collocation [14]. For sufficiently high-permittivity ratios, the ECF approach, even when combined with the Galerkin method, can produce arbitrarily inaccurate results.

In this paper, we show that any numerical scheme directly discretizing the ECF will fail for high-permittivity ratios. The difficulty stems from the fact that the conductor charge, which is of interest, can become much smaller than the charge used to represent the dielectric interface. To resolve this scaling problem, the method described below decomposes the capacitance computation into two problems which are solved consecutively. The first problem corresponds to replacing the finite permittivity dielectric with an infinite permittivity dielectric and involves only large-scale unknowns on the interface. To account for the finite permittivity, a perturbation equation is solved on both surfaces, which only involves small-scale unknowns.

Sections II and III briefly review the ECF as well as some issues for calculating capacitance matrices of multiconductor systems with dielectric materials. The numerical problems that arise for the ECF in the case of high-permittivity ratios are described in Section IV. In Section V, a modification of the existing method is presented, which avoids the difficulties of the ECF. The technique is extended to the multiple conductor case in Section VI and its utility is demonstrated in Section VII by applying our multipole-accelerated implementation of the algorithm to complex multiconductor systems.

Manuscript received October 29, 1997; revised September 21, 1998. This work was supported by the National Science Foundation under Contract ECS-9301-189 and by the DARPA MURI Program.

J. Tausch is with the Department of Mathematics, Southern Methodist University, Dallas, TX 75275 USA (e-mail: tausch@golem.math.smu.edu).

J. White is with the Massachusetts Institute of Technology, Cambridge, MA 02139 USA (e-mail: white@rle-vlsi.mit.edu).

Publisher Item Identifier S 0018-9480(99)00380-4.

II. Boundary Integral Formulation

In inhomogeneous media with permittivity $\varepsilon(x)$, the electrostatic potential ϕ and the electric field $\nabla\phi$ satisfy the boundary value problem

$$\begin{aligned} \nabla^2\phi &= 0, && \text{in } R^3\backslash S \\ \phi &= u, && \text{on } S_c \\ \phi^+ &= \phi^-, && \text{on } S_d \\ \varepsilon^+\frac{\partial\phi^+}{\partial n} &= \varepsilon^-\frac{\partial\phi^-}{\partial n}, && \text{on } S_d \\ \phi &= \mathcal{O}\left(\frac{1}{|x|}\right), && \text{as } |x|\to\infty. \end{aligned} \tag{1}$$

Here, S_c denotes the union of the conductor surfaces, u denotes the given potential on the conductors, S_d is the union of the dielectric interfaces, n is the normal to S_d, and $\phi^\pm = \phi(x \pm 0n)$, $\varepsilon^\pm = \varepsilon(x \pm 0n)$, and $S = S_c \cup S_d$.

Since (1) is an exterior problem, it is advantageous for numerical calculations to cast the differential equation into a boundary integral equation. This is a common approach in electrostatics because the charge density can be calculated directly with this approach. To obtain an integral formulation, write the potential ϕ as the superposition of potentials due to the conductor charge σ_c and the polarization charge on the interface σ_d. In operator notation, this becomes

$$\phi(x) = V_c\sigma_c(x) + V_d\sigma_d(x), \quad x \in R^3. \tag{2}$$

Here, V_c and V_d denote the single-layer potentials on the boundary surfaces S_c and the interfaces S_d, respectively, defined by

$$V_c\sigma_c(x) = \int_{S_c} G(x,x')\sigma_c(x')\,dS_{x'}, \qquad x \in R^3$$

and

$$V_d\sigma_d(x) = \int_{S_d} G(x,x')\sigma_d(x')\,dS_{x'}, \qquad x \in R^3.$$

The kernel $G(x,x')$ is the free-space Green's function for the Laplace operator in three dimensions

$$G(x,x') = \frac{1}{4\pi}\frac{1}{|x-x'|}. \tag{3}$$

Note that the conductor charge σ_c consists of free charges in the conductor and polarization charges in the dielectric material. For the capacitance, only the free charges are important. They are linked to the conductor charge by

$$\sigma_f = \varepsilon^+\sigma_c.$$

The potential defined in (2) satisfies Laplace's equation, is continuous throughout the three space, and decays like $1/|x|$. In order to solve the boundary value problem (1), the potential must also satisfy the boundary conditions on the conductors, as well as the continuity condition on the interfaces. The latter conditions will lead to a system of integral equations for the densities σ_c and σ_d. For that, we must consider the limiting values of $\phi(x)$, defined by (2), as $x \to S$. It is well known that the potential is continuous, but its normal derivative is not continuous across the surface, e.g., [15]. In particular, the following jump relation holds on S_d:

$$\frac{\partial\phi}{\partial n}^{\pm}(x) = K_c'\sigma_c(x) + \left(\mp\frac{1}{2} + K_d'\right)\sigma_d(x), \qquad x \in S_d. \tag{4}$$

Here, the operator K_c' and K_d' denote the normal derivative on the dielectric interface due to the conductor charge and the polarization charge, respectively. They are defined by

$$K_c'\sigma_c(x) = \int_{S_c} \frac{\partial}{\partial n_x}G(x,x')\sigma_c(x')\,dS_{x'}, \qquad x \in S_d$$

and

$$K_d'\sigma_d(x) = \int_{S_d} \frac{\partial}{\partial n_x}G(x,x')\sigma_d(x')\,dS_{x'}, \qquad x \in S_d.$$

Combining (2) and (4) with the boundary conditions of (1), the following system of integral equations for the densities σ_c and σ_d can be derived:

$$\begin{aligned} V_c\sigma_c(x) + V_d\sigma_d(x) &= u(x), \qquad x \in S_c \\ K_c'\sigma_c(x) + \left(\frac{1}{2\lambda} + K_d'\right)\sigma_d(x) &= 0, \qquad x \in S_d. \end{aligned} \tag{5}$$

The parameter λ is given by

$$\lambda = \frac{\varepsilon^- - \varepsilon^+}{\varepsilon^- + \varepsilon^+}. \tag{6}$$

The orientation of the surface normal in (1) and (4) is arbitrary. We will use the convention that the normal of S_d points into the domain of the lower permittivity, which will ensure that $0 < \lambda < 1$.

Subtracting the jump relations (4) from both sides of the surface yields the important relation between the charge density and jump in the normal derivative of the potential

$$\sigma_d = \frac{\partial\phi}{\partial n}^{-} - \frac{\partial\phi}{\partial n}^{+}. \tag{7}$$

Formulation (5) has appeared previously in the literature [6], [7], and is usually referred to as the ECF.

In the following, we will also make use of another relation between the charge density and potential of the capacitance problem. Namely, for the solution ϕ of (1) and σ_c of (5),

$$\int_{R^3} \varepsilon|\nabla\phi|^2 = \int_{S_c} \varepsilon^+\sigma_c u \tag{8}$$

holds. This formula is derived by applying Green's first identity to every connected component of $R^3\backslash S$.

III. Capacitance Matrices

Since the potential on each conductor in an m conductor problem must be constant, $u(x)$ in (5) can be associated with a vector $p \in R^m$. Specifically,

$$u(x) = p_i, \qquad x \in S_{c_i} \tag{9}$$

where S_{c_i} is the surface of the ith conductor. Then, given $u(x)$ associated with a vector p, let $q \in R^m$ be the vector of net-free charges on each conductor, as in

$$q_i = \int_{S_{c_i}} \varepsilon\sigma_c. \tag{10}$$

The capacitance matrix $\mathbf{C} \in R^{m\times m}$ summarizes the relation between the conductor potentials and conductor charges

$$\begin{bmatrix} C_{1,1} & \cdots & C_{1,m} \\ \vdots & \vdots & \vdots \\ C_{m,1} & \cdots & C_{m,m} \end{bmatrix} \begin{bmatrix} p_1 \\ \vdots \\ p_m \end{bmatrix} = \begin{bmatrix} q_1 \\ \vdots \\ q_m \end{bmatrix}. \tag{11}$$

To compute the complete capacitance matrix, it is necessary to solve (5) m times using u's associated with m linearly independent p vectors. An obvious choice for the p vectors is to choose them equal to the m unit vectors. For example, if $p^{(i)}$ is the ith unit vector and $q^{(i)}$ is the resulting vector of conductor charges, then $q^{(i)}$ is the ith column of $\mathbf{C}$. Even though choosing the p vectors to be unit vectors leads to a simple relation between the computed q vectors and columns of the capacitance matrix, we will show in a subsequent section that unit vectors are not always the best choice. For the case of a general set of linearly independent p vectors,

$$\begin{bmatrix} C_{1,1} & \cdots & C_{1,m} \\ \vdots & \vdots & \vdots \\ C_{m,1} & \cdots & C_{m,m} \end{bmatrix} \begin{bmatrix} \vdots & \cdots & \vdots \\ p^{(1)} & \cdots & p^{(m)} \\ \vdots & \cdots & \vdots \end{bmatrix} = \begin{bmatrix} \vdots & \cdots & \vdots \\ q^{(1)} & \cdots & q^{(m)} \\ \vdots & \cdots & \vdots \end{bmatrix}$$

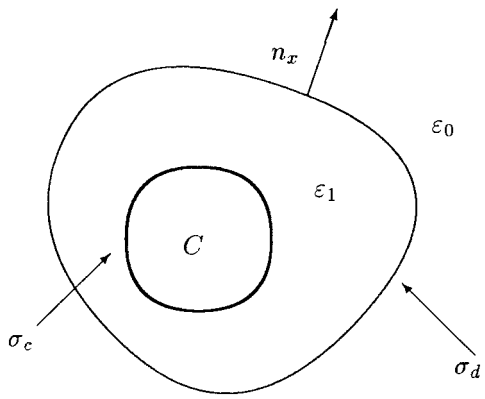

Fig. 1. Inclusion of the conductor C into a dielectric material with permittivity ε_1. The permittivity of the free space is ε_0.

and, therefore, the capacitance matrix can be determined from

$$\begin{bmatrix} C_{1,1} & \cdots & C_{1,m} \\ \vdots & \vdots & \vdots \\ C_{m,1} & \cdots & C_{m,m} \end{bmatrix} = \begin{bmatrix} \vdots & \cdots & \vdots \\ q^{(1)} & \cdots & q^{(m)} \\ \vdots & \cdots & \vdots \end{bmatrix} \begin{bmatrix} \vdots & \cdots & \vdots \\ p^{(1)} & \cdots & p^{(m)} \\ \vdots & \cdots & \vdots \end{bmatrix}^{-1}.$$

IV. High-Permittivity Ratios

Typically, system (5) is discretized with piecewise constant collocation. Numerical experience shows that the error of the approximated capacitances grow rapidly as the ratio of the permittivities increases, e.g., [9]. In the same paper, it is proposed to employ the Galerkin method for the discretization of (5). Even though the Galerkin scheme improves the approximation, the method produces inaccurate results if the permittivity ratio becomes very high. In the following, we will explain why this happens.

To simplify the exposition, we consider a conductor raised to 1 V, which is embedded in a dielectric material, as depicted in Fig. 1. The multiconductor case will be discussed in Section VI.

To study large permittivities, set $\varepsilon_0 = 1$ and let $\varepsilon_1 \to \infty$, which is equivalent to letting λ in (6) approach one. Thus, integral equation (5) reduces to

$$\begin{aligned} V_c\sigma_{c,\infty}(x) + V_d\sigma_{d,\infty}(x) &= 1, \qquad x \in S_c \\ K_c'\sigma_{c,\infty}(x) + \left(\frac{1}{2} + K_d'\right)\sigma_{d,\infty}(x) &= 0, \qquad x \in S_d. \end{aligned} \tag{12}$$

The behavior of the densities $\sigma_{c,\infty}$ and $\sigma_{d,\infty}$ can be determined by examining at the potential

$$\phi_\infty = V_c\sigma_{c,\infty} + V_d\sigma_{d,\infty}$$

generated by the solution of (12). From this integral equation, we see that $\phi_\infty = 1$ on S_c, and by comparing (12) to (4), that $\partial\phi_\infty^-/\partial n = 0$ on S_d. Since ϕ_∞ satisfies Laplace's equation, the potential must be constant within the ε_1 material and the conductor. By (7), the conductor charge $\sigma_{c,\infty}$ vanishes. Since the potential is also one on the dielectric interface, the polarization charge satisfies the integral equation

$$V_d\sigma_{d,\infty}(x) = 1, \qquad x \in S_d. \tag{13}$$

Physically, the $\varepsilon_1 \to \infty$ limit implies that the dielectric material is acting like a conductor. Hence, all charges must be located on the dielectric interface and the conductor charge density must vanish. Equation (13) is equivalent to calculating the capacitance of the structure where the dielectric material has been replaced by a conductor. Thus, the original problem which was posed on S_c and S_d is reduced to a problem posed on S_d only. Moreover, the capacitance of this problem is given by

$$\mathbf{C}_\infty = \int_{S_d} \sigma_{d,\infty}\, dS.$$

Now, consider the densities σ_c, σ_d in the ECF (5) for large, but finite ε_1. Since the solution of the ECF depends continuously on the parameter λ, it is clear that σ_c is small compared to σ_d, because σ_c converges to zero, whereas σ_d converges to the nonzero charge $\sigma_{d,\infty}$.

When solving (5) numerically, the discretization error in the charge density will be distributed evenly over both surfaces, resulting in large relative errors in the computed conductor surface charge. This destroys the accuracy of the capacitance computed using (10) because the inaccurately computed charge density on S_c will be multiplied by ε_1 to calculate the capacitance in (10) and any discretization error will be multiplied by the same factor. On the other hand, the exact value of $\mathbf{C}$ converges to $\mathbf{C}_\infty$. This can be seen by integrating the second equation in (5) over the interface S_d. By Gauss' law, we have $\int_{S_d} K_c'\sigma_c = -\int_{S_c} \sigma_c$ and $\int_{S_d} K_d'\sigma_d = -1/2 \int_{S_d} \sigma_d$. Hence,

$$\mathbf{C} = \int_{S_c} \varepsilon_1\sigma_c = \varepsilon_1\left(\frac{1}{2\lambda} - \frac{1}{2}\right)\int_{S_d} \sigma_{d,\infty} \to \mathbf{C}_\infty. \tag{14}$$

Thus, the discretization error of $\mathbf{C}_\lambda$ grows linearly with ε_1, whereas the exact value remains finite in the limit of $\varepsilon_1 \to \infty$.

V. The Perturbation Approach (PA)

The major numerical difficulty associated with high-permittivity ratios is that the small-scale conductor charge is used to calculate the capacitance. For a single conductor, the self-capacitance could also be calculated via (14) using the polarization charge, thus, avoiding large relative discretization errors. However, the conductor charge density will still be inaccurate and the polarization charge cannot be used to calculate capacitances in multiconductor problems. Instead, we describe here a perturbation technique which allows for accurate estimates of the conductor charge density and extend the approach to the multiconductor case in the following section.

The idea of the PA is to set up the potential as the combination of ϕ_∞, the potential generated by $\varepsilon_1 = \infty$, and the correction $\tilde{\phi}$ accounting for the finite permittivity

$$\phi(x) = \phi_\infty(x) + \tilde{\phi}(x). \tag{15}$$

As was shown above, the potential ϕ_∞ results only from the charge $\sigma_{d,\infty}$ on the interface, which is given by the integral equation (13). This is a capacitance problem in homogeneous media and can be solved numerically to high accuracy [4], [14].

The perturbation $\tilde{\phi}$ is set up as a superposition of charges on the conductor surface and the dielectric interface, similar to the definition of the potential in (2)

$$\tilde{\phi}(x) = V_c\tilde{\sigma}_c(x) + V_d\tilde{\sigma}_d(x). \tag{16}$$

Substituting (16) into (1), one obtains a new set of boundary conditions for the perturbation $\tilde{\phi}$

$$\begin{aligned} \tilde{\phi}(x) &= 0, \qquad x \in S_c \\ \varepsilon^- \frac{\partial \tilde{\phi}}{\partial n}^-(x) - \varepsilon^+ \frac{\partial \tilde{\phi}}{\partial n}^+(x) &= -\varepsilon^+\sigma_{d,\infty}(x), \qquad x \in S_d. \end{aligned} \tag{17}$$

The second equation holds because ϕ_∞ is constant within the dielectric material and, hence, $\partial\phi_\infty^-/\partial n = 0$ and $\partial\phi_\infty^+/\partial n = -\sigma_{d,\infty}$ by the jump relation (7).

These boundary conditions yield, very much in the same way as for (5), the following system of integral equations for the perturbation charges $\tilde{\sigma}_c$ and $\tilde{\sigma}_d$:

$$\begin{aligned} V_c\tilde{\sigma}_c(x) + V_d\tilde{\sigma}_d(x) &= 0 \quad x \in S_c \\ K_c'\tilde{\sigma}_c(x) + \left(\frac{1}{2\lambda} + K_d'\right)\tilde{\sigma}_d(x) &= \frac{\lambda - 1}{2\lambda}\sigma_{\infty,d}(x), \qquad x \in S_d. \end{aligned} \tag{18}$$

Since the potential ϕ_∞ is generated only by charges on the dielectric interface, it follows that $\tilde{\sigma}_c = \sigma_c$. Moreover, the capacitance in (10) reduces to an integral over the perturbation charge

$$\mathbf{C} = \varepsilon_1 \int_{S_c} \tilde{\sigma}_c \, dS. \tag{19}$$

System (18) has the same operator on the left-hand side as the original system (5), only the right-hand side has changed. This is the key observation. The right-hand side scales like $\mathcal{O}(1/\varepsilon_1)$ as $\varepsilon_1 \to \infty$. Hence, by linearity, we see that $\tilde{\sigma}_c$ and $\tilde{\sigma}_d$ are both $\mathcal{O}(1/\varepsilon_1)$ and, therefore, there is no different scaling in the solution of (18).

By the same argument, the error due to discretizing (18) scales like $\mathcal{O}(1/\varepsilon_1)$ for a fixed meshwidth. Hence, the error of the capacitance in (19) can be bounded independently of the permittivity ε_1.

The PA for calculating capacitances of structures involving dielectrics with high permittivities is summarized as follows:

1) solve problem (13) on the interface for $\sigma_{d,\infty}$;
2) solve the perturbation equation (18);
3) calculate the capacitance via (19).

VI. Multiconductor Systems

The technique described above for a single conductor can be generalized to structures consisting of multiple conductors with arbitrary geometries. We illustrate the method with the four conductor structure shown in Fig. 2.

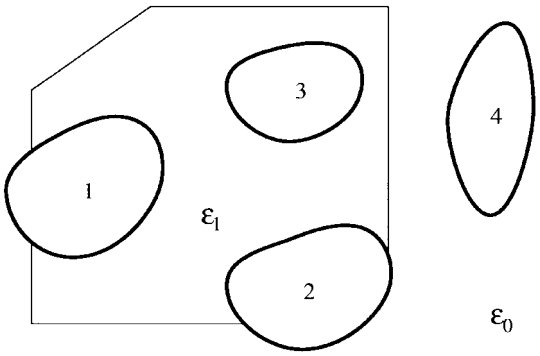

Fig. 2. Multiconductor system. For clarity, conductor surfaces are shown curved, whereas dielectric interfaces are polygonal.

For the limit $\varepsilon_1 \to \infty$, there are two cases that exhibit different behavior of the charge density.

Case 1: Conductors 1–3 have the same potential, $p_1 = p_2 = p_3 = p_0$; the potential on conductor 4 is arbitrary. This case is quite similar to the single conductor case. In the limit $\varepsilon_1 \to \infty$, we have on the interface

$$\frac{\partial \phi}{\partial n}^- \to 0 \tag{20}$$

and it can be seen from (1) that the potential in the dielectric medium approaches the constant value p_0. Thus, the field in the dielectric vanishes and a more careful analysis shows that

$$\int_D |\nabla\phi|^2 = \mathcal{O}(1/\varepsilon_1) \tag{21}$$

where D denotes the region of the ε_1-material. From Green's first identity (8), it follows that for $\mathbf{p} = [p_0, p_0, p_0, p_4]^T$, $p_4 \in R$

$$\frac{\mathbf{p}^T\mathbf{C}\mathbf{p}}{\mathbf{p}^T\mathbf{p}} = \mathcal{O}(1), \qquad \text{as } \varepsilon_1 \to \infty$$

where $\mathbf{C} \in R^{4\times 4}$ is the capacitance matrix defined in (11).

Case 2: Conductors 1–3 have different potentials. In this case, the potential within the dielectric material cannot approach a constant, and

$$\int_D |\nabla\phi|^2 = \mathcal{O}(1), \qquad \text{as } \varepsilon_1 \to \infty \tag{22}$$

and, thus, in view of Green's first identity

$$\frac{\mathbf{p}^T\mathbf{C}\mathbf{p}}{\mathbf{p}^T\mathbf{p}} = \mathcal{O}(\varepsilon_1).$$

Letting $\varepsilon_1 \to \infty$ in the first case corresponds to replacing the dielectric material by a conductor, whereas the limit has no physical meaning for the second case. In fact, as $\varepsilon_1 \to \infty$, the potential energy for the second case approaches infinity.

If the charge density for the first case is calculated via the ECF (5), then the same scaling problem occurs as in the single

conductor case. Because of (7) and (20), the charge density on the conductor surfaces facing the ε_1 material scales like $1/\varepsilon_1$, whereas the polarization charge σ_d approaches a nonzero distribution. Again, the different scaling in the ECF can be avoided with the PA.

The first step is to calculate the charge distribution associated with replacing the ε_1 material by a conductor. For this, remove all ε_1 conductor surfaces. For the structure shown in Fig. 2, conductor 3 and parts of conductors 1 and 2 have to be removed. Furthermore, the interface panels are replaced by conductor panels. The result is a capacitance problem in a homogeneous medium.

As in the single-conductor case, the perturbation charge is obtained by superposition, as in (15). The result is a system of the form (18), whose right-hand side and solution scale like $1/\varepsilon_1$.

If the conductors in the ε_1 material have different potentials, there is no bad scaling in (5) because, in the $\varepsilon_1 \to \infty$ limit, charges must remain on the ε_1 conductor surfaces to maintain a nonconstant potential in the dielectric material. Thus, the charge density can be calculated directly via (5).

Now consider calculating one column of the capacitance matrix of a multiconductor system by raising a conductor to 1 V while grounding the others. For the structure of Fig. 2, one could apply the PA to calculate column $\mathbf{C}_{4,j}$ and the equivalent-charge approach to obtain all other entries. Although this approach avoids different scales in the calculation of each column, there is still a problem. Namely, if $\mathbf{C}$ is used to determine the net charge on the conductors for the potential distribution $\mathbf{p} = [1, 1, 1, 0]^T$, then the resulting charge vector has bad scaling. Hence, the discretization error will scale like ε_1, whereas the charge will approach a finite limit, resulting in large relative errors.

To avoid this problem, calculate $\mathbf{C}$ in a different coordinate system. For this, let $\mathbf{P}_-$ be the matrix whose columns consist of an orthonormal basis of vectors $\mathbf{p}$ whose product $\mathbf{p}^T\mathbf{C}\mathbf{p}/\mathbf{p}^T\mathbf{p}$ remains bounded as $\varepsilon_1 \to \infty$. Furthermore, denote by $\mathbf{P}_+$ the corresponding matrix for the orthogonal complement. The matrices $\mathbf{P}_\pm$ can be determined easily from the problem geometry. For our example, we have

$$\mathbf{P}_- = \begin{bmatrix} \frac{1}{\sqrt{3}} & 0 \\ \frac{1}{\sqrt{3}} & 0 \\ \frac{1}{\sqrt{3}} & 0 \\ 0 & 1 \end{bmatrix} \quad \text{and} \quad \mathbf{P}_+ = \begin{bmatrix} \frac{1}{\sqrt{2}} & \frac{1}{\sqrt{6}} \\ \frac{-1}{\sqrt{2}} & \frac{1}{\sqrt{6}} \\ 0 & \frac{-2}{\sqrt{6}} \\ 0 & 0 \end{bmatrix}.$$

Furthermore, set $\mathbf{Q}_\pm = \mathbf{C}\mathbf{P}_\pm$, $\mathbf{P} = [\mathbf{P}_-, \mathbf{P}_+]$, and $\mathbf{Q} = [\mathbf{Q}_-, \mathbf{Q}_+]$. By linearity of the capacitance problem, the entry $\mathbf{Q}_{i,k}$ is the net charge on conductor i when the potential on the conductors is given by the kth column of $\mathbf{P}$. Thus, $\mathbf{Q}_-$ scales like $\mathcal{O}(1)$ and can be calculated stably using the PA. The matrix $\mathbf{Q}_+$ contains the part of the capacitance matrix that scales like $\mathcal{O}(\varepsilon_1)$ and can be determined directly by the ECF.

Since the matrix $\mathbf{P}$ is orthonormal, $\mathbf{P}^{-1} = \mathbf{P}^T$ and

$$\mathbf{C}' = \mathbf{P}^T\mathbf{C}\mathbf{P} = \mathbf{P}^T\mathbf{Q}$$

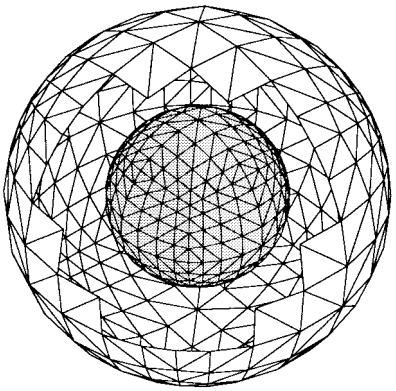

Fig. 3. The coated sphere. Some of the interface panels have been removed to show the inner conductor surface panels.

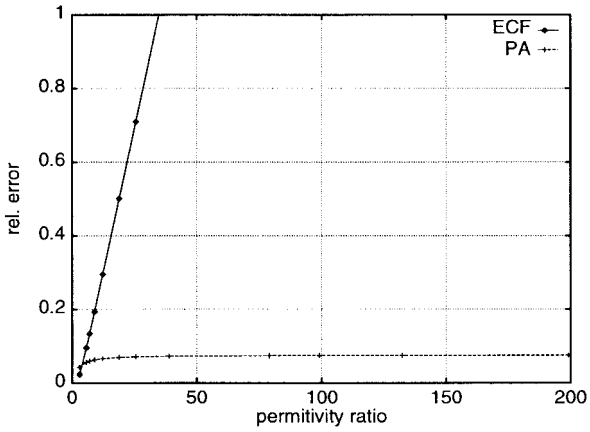

Fig. 4. Relative errors of the capacitance as calculated by the ECF and the modified formulation. Coated-sphere example. The exact value of the capacitance varies between 18–25.

TABLE I
NUMBER OF GMRES ITERATIONS REQUIRED TO SOLVE THE EQUIVALENT-CHARGE FORMULATION ANDTHE PERTURBATION EQUATION FOR THE COATED-SPHERE PROBLEM

ε_1	2	5	10	20	50	100	1,000
ECF	7	7	7	7	7	7	7
PA	8	8	8	8	8	8	8

is a similarity transform of $\mathbf{C}$. The capacitance-matrix matrix can be determined by calculating the matrix $\mathbf{Q}$ first and then recovering $\mathbf{C}$ from

$$\mathbf{C} = \mathbf{P}\mathbf{C}'\mathbf{P}^T = \mathbf{Q}\mathbf{P}^T.$$

VII. RESULTS

To demonstrate the accuracy and stability of the PA described in this paper, we compare the capacitances obtained by the PA, ECF, and other approaches for several structures and permittivity ratios. While the first three examples illustrate the solution behavior for simple geometries, the last two examples are included to demonstrate that the PA can be useful for more realistic and complex structures.

The problems were discretized with piecewise constant collocation and the arising linear systems were solved using

TABLE II
CONVERGENCE BEHAVIOR, TWO SPHERES IN ELLIPSOIDAL DIELECTRIC MEDIUM. NOTE THAT FOR $p = [1, -1]$, THE ECF AND THE PA GIVE THE SAME RESULTS

	$\varepsilon = 10$				$\varepsilon = 100$				$\varepsilon = 1000$			
Panels	576	2304	9216	36864	576	2304	9216	36864	576	2304	9216	36864
$\mathbf{C}_{\mathrm{PA}}\begin{bmatrix}1\\1\end{bmatrix}$	8.018	8.623	8.893	9.025	8.567	9.307	9.652	9.826	8.627	9.384	9.738	9.917
	5.109	5.496	5.675	5.765	5.544	6.034	6.273	6.396	5.592	6.096	6.341	6.469
$\mathbf{C}_{\mathrm{ECF}}\begin{bmatrix}1\\1\end{bmatrix}$	11.82	10.86	10.11	9.649	52.96	35.79	24.21	17.30	459.5	278.8	158.0	86.05
	7.543	6.936	6.465	6.170	34.46	23.40	15.87	11.34	299.8	183.1	104.2	56.90
$\mathbf{C}_{\mathrm{ECF}}\begin{bmatrix}1\\-1\end{bmatrix}$	49.57	50.58	50.50	50.29	449.5	454.9	451.5	448.0	4446	4494	4457	4420
	−45.35	−46.69	−46.87	−46.82	−431.7	−442.9	−443.4	−442.1	−4293	−4403	−4406	−4392

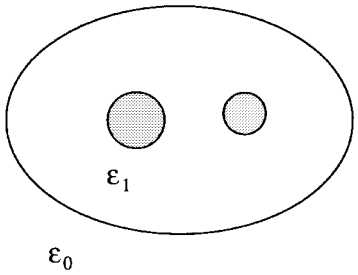

Fig. 5. Two spheres in a dielectric medium.

the iterative solver GMRES. To accelerate the matrix-vector products, the fast multipole algorithm was applied, [2], [5]. Our code is based on the package FASTCAP [4] with some modifications to calculate the normal derivatives of the potential for the interface condition. The results are displayed dimension-free, i.e., $\varepsilon_0 = 1$.

A. Coated Sphere

In the first example, we approximate the capacitance of the unit radius spherical conductor, which is covered by a concentric-unit thick coating with discretization, as shown in Fig. 3.

Due to the spherical geometry, the analytic value of the capacitance is known. The same discretization into 1536 panels was used to approximate the capacitance with the ECF and by the perturbation method for a wide range of permittivity ratios.

Fig. 4 compares the discretization errors obtained from both formulations. As can be seen from this plot, the equivalent-charge approach gives enormous discretization errors for high-permittivity ratios, whereas the error of the PA remains small, even when $\varepsilon_1 \to \infty$.

The condition number for a fixed discretization is bounded as the permittivity ratio is increased. This is true for both formulations. The reason is that the ECF (5) converges in the limit $\lambda \to 1$ to the well-posed integral equation (12). As a result, the number of GMRES iterations to solve the discretized linear systems is independent of the permittivity. This is demonstrated for the coated sphere in Table I. For the other structures, the iterative method took more steps to converge, but showed the same independence of the permittivity. This again makes it clear that the accuracy problem of the ECF is not ill conditioning, but a scaling problem.

B. Two Spheres in a Dielectric Medium

The second structure consists of two spheres in an ellipsoidal dielectric medium, as shown in Fig. 5. The defining equations for the conductors and the interface are

$$x_1^2 + \left(x_2 + \frac{3}{4}\right)^2 + x_3^2 = \frac{1}{4}$$

$$\left(x_1 - \frac{1}{5}\right)^2 + \left(x_2 - \frac{4}{5}\right)^2 + \left(x_3 - \frac{1}{5}\right)^2 = \frac{1}{3}$$

$$x_1^2 + x_2^2 + \frac{9}{4}x_3^2 = \frac{9}{4}$$

respectively. As there is no closed-form solution for this problem, we investigate the behavior of the numerical approximation for different mesh refinements. To make the differences between conductors at equal and different potentials clear, we show in Table II the computed net-free charges for potential vectors $p = [1, 1]^T$ and $p = [1, -1]^T$.

In the equal potential case, there is a significant difference in the convergence behavior of the ECF and PA. For all permittivities calculated, the net charges obtained using the PA and the 2304 panel grid are within 5%-6% of the corresponding values obtained from the finest grid. On the other hand, the ECF requires for $\varepsilon = 10$ a finer discretization into 9216 panels to be within 5% of the finest grid result. For larger permittivities, even the finest grid results of the ECF have not converged within reasonable accuracy.

Contrary to the equal potential case, the ECF provides accurate results for any permittivity ratio if the conductors are at different potentials. It can be seen from the table that all approximations using the 2304 panel grid are within 1% of the finest grid. This demonstrates that the bad scaling of the equal potential case is the sole source of error in the ECF.

C. Comparison with Modified Green's Function

The main purpose of the ECF and PA is to handle arbitrary distributions of dielectric materials. However, the case of layered media is common and modified Green's functions are an alternative to the ECF or PA. For a single dielectric interface

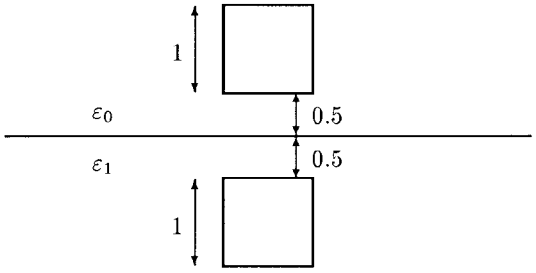

Fig. 6. Cross-sectional view of two cubes in a layered medium.

TABLE III
COMPARISON OF CAPACITANCES FOR FIG. 6 AS CALCULATED BY MODIFIED GREEN'S FUNCTIONS PERTURBATION APPROACH AND ECF. NOTE THAT FOR $p = [0, 1]$, THE ECF AND PA GIVE THE SAME RESULTS

	$p = [1, 0]^T$			$p = [0, 1]^T$	
	MG	PA	ECF	MG	ECF
$\varepsilon = 10$	11.94	11.92	11.86	−5.658	−5.584
	−5.658	−5.639	−6.416	68.42	69.17
$\varepsilon = 100$	12.44	12.43	12.35	−6.162	−6.073
	−6.162	−6.141	−15.31	633.8	642.8
$\varepsilon = 1000$	12.49	12.48	12.40	−6.218	−6.127
	−6.218	−6.196	−99.42	6282	6374

at $x_3 = 0$, the Green's function can be found by the method of images

$$G_\varepsilon(x,x') = \begin{cases} \dfrac{1}{\varepsilon_0}\left(G(x,x') - \dfrac{\varepsilon_1-\varepsilon_0}{\varepsilon_0+\varepsilon_1}G(x,Px')\right), & x_3, x_3' > 0 \\ \dfrac{2}{\varepsilon_1+\varepsilon_0}G(x,x'), & x_3 \cdot x_3' < 0 \\ \dfrac{1}{\varepsilon_1}\left(G(x,x') - \dfrac{\varepsilon_0-\varepsilon_1}{\varepsilon_1+\varepsilon_0}G(x,Px')\right), & x_3, x_3' < 0 \end{cases}$$

where $G(x,x')$ is the free-space Green's function defined in (3) and Px is the image of x. Thus the capacitance problem reduces to solving

$$\int_{S_c} G_\varepsilon(x,x')\sigma_f(x')\,dS_{x'} = u(x), \quad x \in S_c \tag{23}$$

on the conductor surfaces.

In this example, we consider two cubes above and below the interface, as indicated in Fig. 6, where $\varepsilon_0 = 1$.

For the modified Green's function, each cube was discretized into 600 rectangular panels. In addition, for the ECF and PA, the interface was truncated to a square plate of sidelength 12 and discretized into 784 panels.

Different from the case of a finite dielectric, only a potential that vanishes on the bottom conductor will generate a badly scaled density. If the potential is nonzero in the high-permittivity region, the charge density on the bottom conductor will not converge to zero as $\varepsilon_1 \to \infty$.

This suggests to use the PA only for the first column of the capacitance matrix. The results in Table III demonstrate that the capacitances calculated this way are in good agreement with the capacitances obtained from the modified Green's function approach. As expected, the ECF produces highly erroneous results when the permittivity ratio gets large.

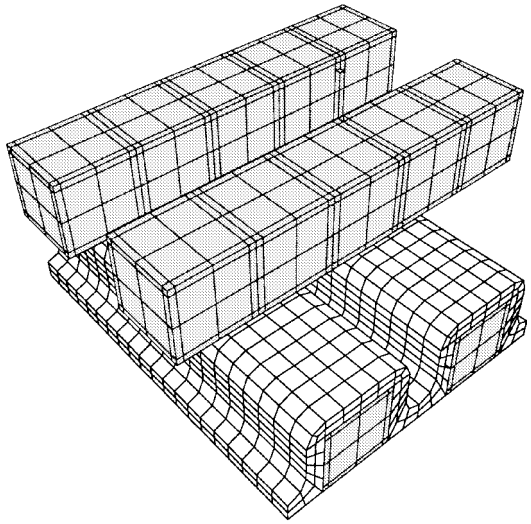

Fig. 7. Bus-crossing example, the lower conductors are covered by a dielectric material. Discretization used in the calculations is finer than shown.

If the top conductor is grounded and the bottom conductor has a nonzero potential, then there is no bad scaling in the solution and the numerical approximation obtained by the ECF are in good agreement with those obtained by the modified Green's function approach.

D. Bus Crossing

To demonstrate that the PA is also useful for complex multiconductor systems, the capacitance matrix associated with the bus-crossing structure of Fig. 7 is calculated.

All the conducting bars have 1×1units cross sections. Conductors 1 and 2 are covered by a dielectric material whose thickness is approximately 0.25 units. The spacing between the conductors in the horizontal direction is 0.4 units and 1 unit in the vertical direction. The structure was discretized into 10 400 panels, out of which 4768 panels were placed on the dielectric interface.

The capacitance matrices calculated by both methods are compared in Tables IV and V. As expected, the results of both approaches are close for a small permittivity. The effect of the bad scaling in the ECF becomes obvious for the coupling capacitances between the top and bottom conductors when $\varepsilon_1 = 10$. The matrices of the ECF are far from symmetric, even though a fine discretization was used. For the PA, there is still asymmetry, however, it is much smaller and does not grow when ε_1 is increased.

E. Connector

The capacitances associated with the backplane connector of Fig. 8 are investigated in Table VI. For $\varepsilon_1 = 10$, the results of both methods appear to be close. However, the differences become obvious if the capacitance matrix is used to determine the net charges on the pins for a constant potential. From (8), it is clear that the net charges for this case must remain bounded in the limit $\varepsilon_1 \to \infty$. The results obtained by the PA

TABLE IV
COMPARISON OF THE CALCULATED CAPACITANCE MATRIX FOR THE BUS CROSSING IN FIG. 7. TOP: EQUIVALENT-CHARGE FORMULATION, BOTTOM: PERTURBATION METHOD. $\varepsilon_1 = 2$

$$\mathbf{C}_{\mathrm{ECF}} = \begin{bmatrix} 44.32 & -12.15 & -12.26 & -12.26 \\ -12.14 & 44.32 & -12.26 & -12.27 \\ -12.21 & -12.21 & 39.42 & -8.19 \\ -12.21 & -12.21 & -8.187 & 39.42 \end{bmatrix}$$

$$\mathbf{C}_{\mathrm{PA}} = \begin{bmatrix} 44.14 & -12.33 & -12.14 & -12.14 \\ -12.33 & 44.14 & -12.14 & -12.14 \\ -12.30 & -12.30 & 39.56 & -8.175 \\ -12.30 & -12.30 & -8.175 & 39.56 \end{bmatrix}$$

TABLE V
COMPARISON OF THE CALCULATED CAPACITANCE MATRICES FOR THE BUS CROSSING IN FIG. 7. TOP: EQUIVALENT-CHARGE FORMULATION, BOTTOM: PERTURBATION METHOD. $\varepsilon_1 = 10$

$$\mathbf{C}_{\mathrm{ECF}} = \begin{bmatrix} 75.38 & -30.12 & -18.01 & -18.00 \\ -30.11 & 75.37 & -18.01 & -18.00 \\ -16.67 & -16.67 & 47.46 & -7.702 \\ -16.67 & -16.67 & -7.702 & 47.46 \end{bmatrix}$$

$$\mathbf{C}_{\mathrm{PA}} = \begin{bmatrix} 73.24 & -32.26 & -16.43 & -16.44 \\ -32.24 & 73.25 & -16.45 & -16.45 \\ -16.90 & -16.90 & 47.85 & -7.68 \\ -16.90 & -16.90 & -7.679 & 47.85 \end{bmatrix}$$

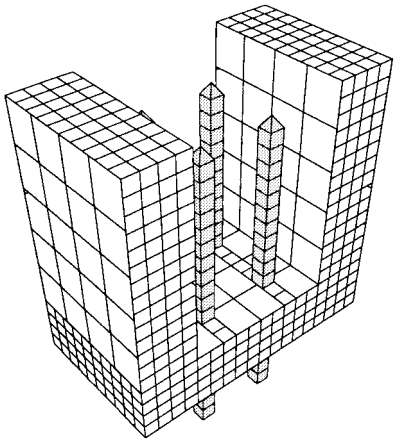

Fig. 8. Backplane connector with four pins. Discretization used in the calculations is finer than shown.

reflect this behavior well, whereas the net charges of the ECF increase without bounds.

F. Central Processing Unit (CPU) Timing

The perturbation method involves solving an additional capacitance problem for the infinite permittivity case. Since this problem is always less complex than the original capacitance problem, the overall CPU time of the PA is less than twice the time of the ECF. The actual factor varies with the problem geometry and Table VII displays the timings for our examples. Our current implementation of the perturbation method restarts the whole calculation for the perturbation equation. Further optimizations could be achieved by reusing already calculated data of the infinite permittivity problem.

TABLE VI
COMPARISON OF THE CALCULATED CAPACITANCE MATRICES FOR THE CONNECTOR OF FIG. 8. $\varepsilon_1 = 10$

$$\mathbf{C}_{\mathrm{ECF}} = \begin{bmatrix} 170.0 & -54.29 & -60.28 & -20.82 \\ -54.24 & 169.9 & -20.82 & -60.16 \\ -60.34 & -20.83 & 170.2 & -54.28 \\ -20.85 & -60.32 & -54.22 & 170.2 \end{bmatrix}$$

$$\mathbf{C}_{\mathrm{ECF}} \cdot \begin{bmatrix} 1 \\ 1 \\ 1 \\ 1 \end{bmatrix} = \begin{bmatrix} 34.65 \\ 34.71 \\ 34.72 \\ 34.80 \end{bmatrix}$$

$$\mathbf{C}_{\mathrm{PA}} = \begin{bmatrix} 168.1 & -56.21 & -62.20 & -22.73 \\ -56.17 & 168.0 & -22.74 & -62.09 \\ -62.28 & -22.77 & 168.2 & -56.22 \\ -22.79 & -62.27 & -56.17 & 168.2 \end{bmatrix}$$

$$\mathbf{C}_{\mathrm{PA}} \cdot \begin{bmatrix} 1 \\ 1 \\ 1 \\ 1 \end{bmatrix} = \begin{bmatrix} 26.98 \\ 27.01 \\ 26.96 \\ 27.02 \end{bmatrix}$$

TABLE VII
TOTAL CPU TIMES IN MINUTES, $\varepsilon_1 = 10$

	Sphere	Connector	Bus
# Panels	1,536	2,960	10,400
ECF	0:35	2:16	16:46
PA	0:45	3:16	25:42

VIII. CONCLUSION

The capacitance calculation for structures with multiple dielectrics by the ECF can be erroneous when the ratio of the permittivities is high. The error is due to bad scaling of the solution and not due to ill conditioning of the integral formulation. The PA described in this paper does not suffer from an accuracy loss in this case. Furthermore, calculations with the new approach can be multipole accelerated and are, therefore, efficient enough to allow capacitance extractions of complex 3-D, multiple-dielectric geometries.

Finally, perturbation methods can also be applied to structures containing more than two dielectrics with high-permittivity ratios, e.g., when $\varepsilon_0 = 1$, $\varepsilon_1 = 10$, and $\varepsilon_2 = 100$. However, the approach gets more involved, sometimes requiring the solution of two or more perturbation equations. Although it is often easy to tell what to do for a given structure, the description of the most general case is complicated and beyond the scope of this paper.

REFERENCES

[1] R. F. Harrington, *Field Computation by Moment Methods*. New York: Macmillan, 1968.

[2] L. Greengard, *The Rapid Evaluation of Potential Fields in Particle Systems*. Cambridge, MA: MIT Press, 1988.

[3] S. Kapur and J. Zhao, "A fast method of moments solver for efficient parameter extraction of MCM's," in *Design Automation Conf.*, Anaheim, CA, June 1997.

[4] K. Nabors and J. White, "Fastcap: A multipole accelerated 3-D capacitance extraction program," *IEEE Trans. Computer-Aided Design*, vol. 11, pp. 1447–1459, 1991.

[5] V. Rokhlin, "Rapid solution of integral equations of classical potential theory," *J. Comput. Phys.*, vol. 60, no. 2, pp. 187–207, 1985.

[6] A. Ruehli, "Survey of computer-aided electrical analysis of integrated circuit interconnections," *IBM J. Res. Develop.*, vol. 23, no. 6, pp. 626–639, 1973.

[7] S. Rao, T. Sarkar, and R. Harrington, "The electrostatic field of conducting bodies in multiple dielectric media," *IEEE Trans. Microwave Theory Tech.*, vol. MTT-32, pp. 1441–1448, 1984.

[8] K. Nabors and J. White, "Multipole-accelerated capacitance extraction algorithms for 3-D structures with multiple dielectrics," *IEEE Trans. Circuits Syst.*, vol. 39, pp. 946–954, 1992.

[9] X. Cai, K. Nabors, and J. White, "Efficient Galerkin techniques for multipole-accelerated capacitance extraction of 3-D structures with multiple dielectrics," in *Proc. Conf. Advanced Res. VLSI*, Chapel Hill, NC, 1995.

[10] C. Wei, R. F. Harrington, J. R. Mautz, and T. K. Sarkar, "Multiconductor transmission lines in multilayered dielectric media," *IEEE Trans. Microwave Theory Tech.*, vol. MTT-32, pp. 439–449, 1984.

[11] K. Li, K. Atsuki, and T. Hasegawa, "General analytical solutions of static Green's functions for shielded and open arbitrary multilayered media," *IEEE Trans. Microwave Theory Tech.*, vol. 45, pp. 2–8, Jan. 1997.

[12] V. Jandhyala, E. Michielssen, and R. Mittra, "Multipole-accelerated capacitance computation for 3-D structures in a stratified dielectric medium using a closed form Green's function," *Int. J. Microwave Millimeter-Wave Computer-Aided Eng.*, vol. 5, no. 2, pp. 68–78, 1995.

[13] J. R. Phillips and J. White, "Efficient capacitance extraction of 3D structures using generalized pre-corrected FFT methods," in *Proc. IEEE 3rd Topical Meeting Electrical Performance Electron. Packag.*, Monterey, CA, Nov. 1994.

[14] A. Ruehli and P. Brennan, "Efficient capacitance calculations for three-dimensional multiconductor systems," *IEEE Trans. Microwave Theory Tech.*, vol. MTT-2, pp. 76–82, Jan. 1973.

[15] R. Kress, *Linear Integral Equations*, vol. 82 of *Applied Mathematical Sciences*. Berlin, Germany: Springer-Verlag, 1989.

Johannes Tausch received the Diplom (M.S. degree) from Julius Maximilians University, Wuerzburg, Germany, and the Ph.D. degree in mathematics from Colorado State University, Fort Collins, in 1995.

After completing post-doctoral work at the Research Laboratory of Electronics, Massachusetts Institute of Technology, Cambridge, he became an Assistant Professor at Southern Methodist University, Dallas, TX. His research interests include numerical approximations and fast solution methods for boundary integral equations with applications to computational electromagnetics.

Jacob White (A'88) received the B.S. degree in electrical engineering and computer science from the Massachusetts Institute of Technology (MIT), Cambridge, and the S.M. and Ph.D. degree in electrical engineering and computer science from the University of California at Berkeley.

From 1985 to 1987, he worked at the IBM T. J. Watson Research Center. From 1987 to 1989, he was an Analog Devices Career Development Assistant Professor at the Massachusetts Institute of Technology. He is currently a Professor at MIT. His research interests are in serial and parallel numerical algorithms for problems in circuit, interconnect, device, and microelectromechanical system design.

Dr. White was an associate editor of the IEEE TRANSACTIONS ON COMPUTER-AIDED DESIGN from 1992 to 1996. He was a 1988 Presidential Young Investigator.